Effect of Shear Flow on the Morphology and Phase Behavior of a Near-Critical SAN/PMMA Blend

Zhengyu Hong,[†] Montgomery T. Shaw,*[,†,‡] and R. A. Weiss[†,‡]

Polymer Program and Department of Chemical Engineering, University of Connecticut, Storrs, Connecticut 06269

Received April 22, 1998; Revised Manuscript Received June 29, 1998

ABSTRACT: An ongoing debate concerns whether experimental observations of flow-induced miscibility of polymer blends actually result from a "true" shift of the critical temperature. To elucidate the origin of the phenomenon more clearly, we have investigated the structural changes of phase domains of a number of polymer blends under the influence of flow. The most recent study used a near-critical blend of poly(styrene-*co*-acrylonitrile)/poly(methyl methacrylate), which exhibits LCST type phase behavior. Rheo-SALS (small angle light scattering) was used to probe the time-dependent structure evolution during shear flow. Quenched samples were examined with TEM and phase contrast light microscopy, and the Fourier transforms of digitized micrographs were compared with two-dimensional light scattering measurements of the same samples. The blends were also subjected to pressure-driven flows and drag flows at very high stresses, and their morphology was similarly studied. The structure evolution due to flow could be explained by hydrodynamic effects consistent with droplet breakup theory.

Introduction

The pronounced influence of shear deformation on the phase behavior of polymer blends offers an opportunity for morphology control during processing.[1] Ever since the description in 1952 of shear-induced phase changes in polymer solutions,[2] phase transitions and critical phenomena of polymer solutions and blends have been the subject of extensive theoretical and experimental investigation. A number of authors[3−16] have suggested that flow can induce changes in the degree of mixing by influencing the thermodynamic state of polymer blends; i.e., flow shifts the phase transition temperatures. Recent studies, however, indicate that this is not the case[17−21] and that hydrodynamic effects are responsible for the observations.

The objective of our study was to investigate the transient structural changes of phase domains in SAN/PMMA blends at high stresses in a number of different flows in order to gain a better understanding of what occurs with the blend morphology and phase behavior. Most studies have used the discontinuity of the viscosity, turbidity, or concentration fluctuations as evidence of a first-order phase transition. In contrast, the morphology of the blends has been largely neglected. The SAN/PMMA system was chosen because the high T_g's of the two polymers and the narrow temperature gap between the cloud point and T_g make it relatively easy to quench the blend from the melt so as to preserve the microstructure for closer examination. One earlier study of this blend[5] produced the conclusion that stress can markedly increase miscibility. Our results described below, however, indicate that the effect of flow is more complex, and it may be qualitatively explained by hydrodynamic deformation, agglomeration, and breakup of phase-separated droplets or flow instabilities in the melt. The results at this point are limited to one blend and thus could be unique to this blend. Other blends will be discussed in future reports.

[†] Polymer Program.
[‡] Department of Chemical Engineering.

Table 1. Characteristics of Components and Blend

polymer	wt %	T_g, °C	n_D @ 20 °C	M_w, kDa	M_w/M_n
SAN (29% AN)	25	105	1.57	108	2.32
PMMA	75	107	1.49	92	1.87

Experimental Section

Materials. A binary mixture of poly(styrene-*co*-acrylonitrile) (SAN) and poly(methyl methacrylate) (PMMA) with a near-critical composition of 25/75 SAN/PMMA was used. Characteristics of the components are listed in Table 1. The SAN/PMMA blend exhibited a lower critical solution temperature[22] (LCST) type phase diagram. The cloud-point temperature (T_{cp}) of the 25/75 SAN/PMMA blend was determined by using a custom-built light scattering instrument[23] to be 168 °C. Mixtures were prepared by melt mixing at 150 °C in a Brabender Plasticorder. Well-mixed blends were compression molded into 0.8-mm-thick sheets at 150 °C, and 50-mm-diameter disks were cut for rheo-SALS studies. Gel permeation chromatography measurements of the polymer molecular weights before and after shear-flow indicated that no degradation occurred under the conditions used for the rheo-SALS experiments.

Rheo-SALS Measurements. Time-resolved small angle light scattering measurements were performed with a custom-built rheo-SALS apparatus.[24] The instrument uses a Rheometrics mechanical spectrometer for controlling the shear flow between 50-mm-diameter parallel plates. Light is provided by a 10-mW He−Ne laser. The scattering image of the flowing melt is projected onto a semitransparent screen, and the image is recorded with a Princeton Instruments 2-D CCD camera.

The blend was heated to 12 °C above T_{cp} (180 °C) between the parallel plates of the rheo-SALS instrument until the sample was well phase-separated. Shear was then applied and the time-resolved 2-D light scattering patterns were recorded. Shear was stopped after several hours (depending on the shear rate applied) when a steady state was reached; i.e., the scattering pattern did not change with strain. Shear rates were limited to 0.01−0.05 s^{-1} because secondary flows occurred at higher rates. The corresponding shear stresses were below 60 kPa. When the shearing was stopped, the sample was quickly quenched to below the glass transition temperature to preserve the morphology, which was then characterized by phase-contrast optical microscopy. Light scattering patterns of the microscopy specimens were also obtained using a simple

S0024-9297(98)00637-8 CCC: $15.00
Published on Web 08/21/1998

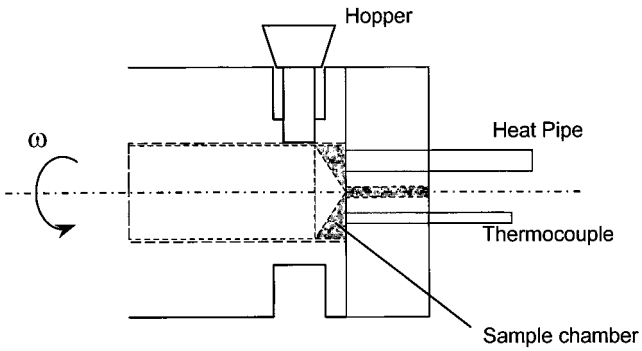

Figure 1. Schematic drawing of the modified CSI normal-stress extruder.

setup with a He−Ne laser ($\lambda = 632.8$ nm) and a 35-mm camera to record the scattered light imaged on a semitransparent screen.

Another set of experiments was carried out wherein steady shear was applied to the melt at 160 °C, which is within the one-phase region of the quiescent phase diagram. The purposes of this exercise were to check for instrumental artifacts and to see if the flow perturbed the structure of the miscible blend melt. The light scattering pattern of the sheared blend was monitored while the temperature was raised at a heating rate of 0.2 °C/min. The phase-separation temperature was defined as the point at which anisotropy in the scattering pattern first appeared.

High-Rate Pressure-Driven and Drag Flows. Melt flow behavior of the blends in the shear rate range 0.3−200 s^{-1} was determined using an Instron Capillary Rheometer. The capillaries used had aspect ratios (L/D) of 20 and 40 with diameters of 0.1 and 0.05 in., respectively, and the Bagley end correction was determined to be negligible. The Rabinowitsch correction was applied in calculating the wall shear rate.

Extrudates of the SAN/PMMA blend at 180 °C were quenched in iced water as soon as they exited the die. The quenched strands were then microtomed both normal and parallel to the flow direction. A Philips-300 transmission electron microscope was used to image the microtomed specimens. Staining was not necessary because the contrast between the SAN- and PMMA-rich domains was sufficient to distinguish the two phases, with the dark and light regions of the micrographs presented here corresponding to SAN-rich and PMMA-rich, respectively.

For high-stress drag flow, a CSI normal-stress extruder, modified with a flush-mounted heat pipe, was used. A schematic drawing of the instrument was shown in Figure 1. The polymer melt inside the extruder and near the heat pipe was rapidly quenched by spraying the exterior of the heat pipe with ice water. The temperature was read from a thermocouple mounted downstream at the same radius as the heat pipe. The extruder had a cone and plate configuration, so that the flow was roughly homogeneous. Various shear rates from 5 to 12 s^{-1} were applied by adjusting the rotational speed. By starve feeding the extruder, we achieved much longer residence times for the blend than were possible in the capillary rheometer, even without closing the die. The morphology of quenched samples was determined in the same way as for the capillary extrudates.

Image Analysis. The number-average equivalent diameter of the domains in the optical micrographs was calculated using Microgop 2000 image analysis software. Two-dimensional spatial Fourier transforms (FT) of the images were also produced using this program.

Results and Discussion

Rheo-SALS. The phase-separated 25/75 SAN/PMMA blend exhibited a common trend of time-dependent structure evolution at the various shear stresses studied. The structure proceeded from a bicontinuous one, to a chevron-like structure, and eventually to a fibrillar morphology, as shown in Figure 2, column A. Columns B, C, and D are the corresponding real-time scattering patterns, scattering patterns for the quenched samples, and Fourier transforms (FT) of the micrographs, respectively.

The quiescent blend underwent spinodal decomposition at 12 °C above T_{cp}. A typical bicontinuous phase structure observed by optical microscopy is shown in Figure 2A(1); the average domain size (characteristic length) was ca. 0.7 μm. The corresponding real-time light scattering patterns for this structure, Figure 2B-(1), show a spinodal ring at a scattering vector $q = (4n_0\pi/\lambda)\sin(\theta/2)$ (λ is the light wavelength = 0.6328 μm, θ is the scattering angle, and n_0 is the refractive index of the medium), of 9.1 μm^{-1}. The domain size and scattering vector are related through Bragg's law,

$$\xi = 2\pi/q \tag{1}$$

where ξ is the characteristic length of the domain and q is the scattering vector magnitude. Both the light scattering patterns for the quenched samples and the FT of the digitized micrographs were consistent with the corresponding real-time light scattering patterns.

When a shear strain of $\gamma = 8$ was applied to the sample at 0.02 s^{-1}, a unique chevron-like phase structure formed, see Figure 2A(2). The phases were oriented in a zigzag pattern with a distribution of tilt angles relative to the flow direction. The angles became smaller with increasing strain. In reciprocal space, the scattering intensity grew in the flow direction and gradually developed into a pattern of two "wings" separated by a dark gap oriented perpendicular to the flow, Figure 2B(2). The dark streak (the gap) narrowed with increasing shear strain, indicating an increase of the characteristic length in the flow direction. Careful examination of the chevron structure by optical sectioning under the microscope revealed the same pattern from one surface of the sample to the other. A single-component polymer sample subject to the same treatment did not show any chevron structure, suggesting that the pattern was not due to a surface flow instability. The formation of the chevron structure may be due to a nonaffine deformation of a highly interconnected spinodal structure and the high viscosity of the blend at this temperature. Further investigation of this very local flow inhomogeneity is continuing.

As the shear strain increased further, the phase domains continued to deform and elongate along the flow direction, forming a fibrillar structure, Figure 2A-(3). The scattering intensity increased significantly and the dark streak disappeared gradually from lower to higher scattering vectors. Eventually, a bright-streak scattering pattern was observed, Figure 2B(3), and that scattering pattern did not change with time. Similar fibrillar, string-like, structures have been reported in the literature to form before a phase transition occurs.[25,26] However, in our study, this structure persisted even after shearing for 24 h.

The light scattering patterns of the microscopy samples and the corresponding FT's shown in Figure 2C,D, confirm that the microstructures preserved in the quenched specimens were the same as that in the real-time rheo-SALS experiments. The results shown in Figure 2 clearly demonstrate the time dependency of the shear-induced changes in the phase structure of a blend. No shear-induced phase transitions were ob-

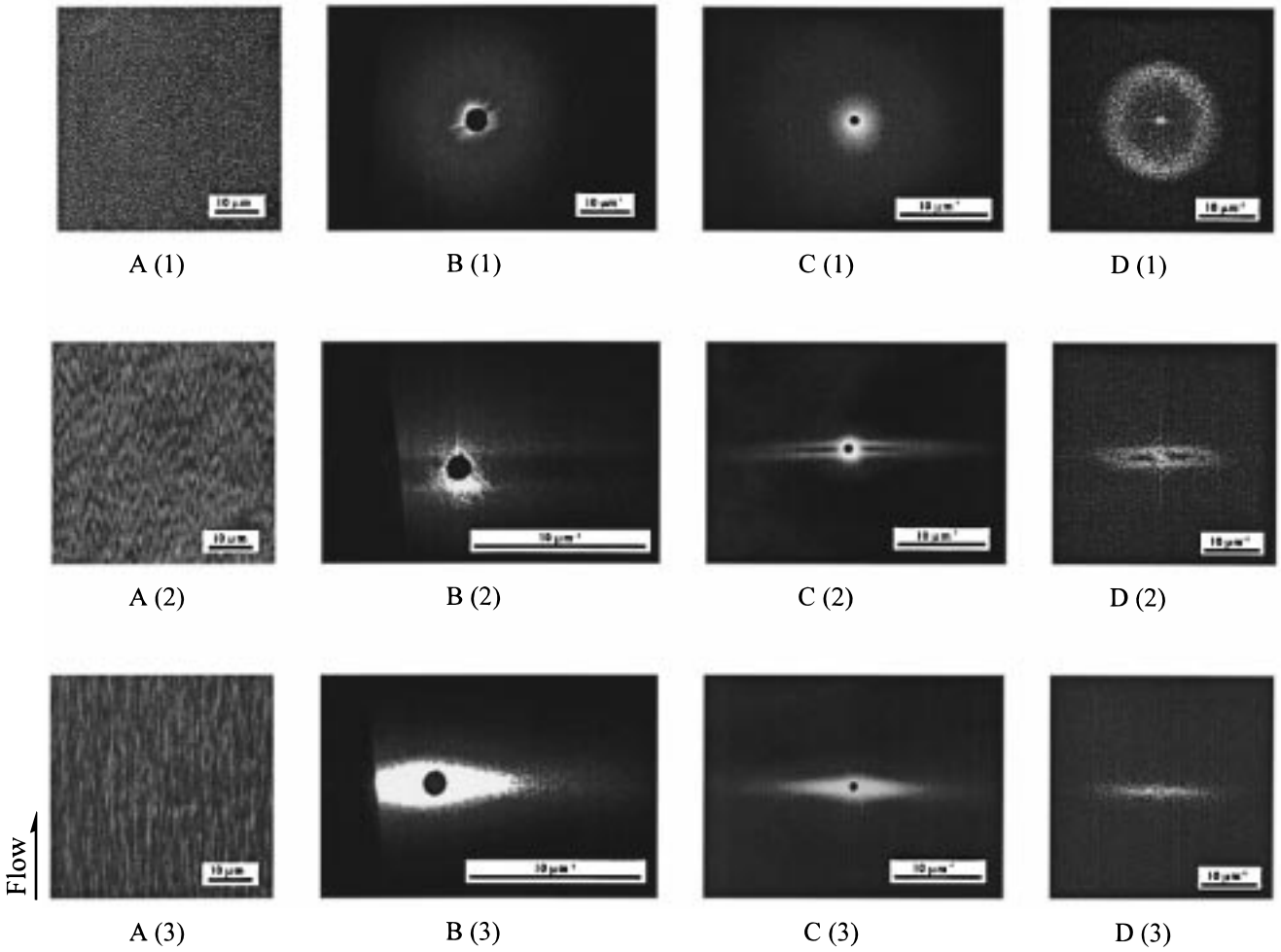

Figure 2. Microstructure of 25/75 SAN/PMMA and their corresponding light scattering patterns and FT spectra after shearing at 0.02 s^{-1}. Column: (A) micrographs using optical microscopy; (B) real-time 2D LS patterns using rheo-SALS; (C) LS pattern using quenched samples; (D) FT of digitized micrographs. Row: (1) $\gamma = 0$; (2) $\gamma = 8$; (3) $\gamma = 288$.

served for shear stresses up to 60 kPa, despite the fact that when the shear was applied, the blend became optically clearer; i.e., the turbidity of the system decreased. This was especially true at high shear stresses. However, the data in Figure 2 indicate that the turbidity changes were due to alignment and stretching of phase domains in the flow direction and not flow-induced mixing, as has been concluded from some previous investigations based on changes in the turbidity of blends undergoing shear flow.[8,12,16] The very thin domains produced by shear flow scatter much less light, which indicates that turbidity (or even scattering at a particular angle) is not a conclusive indicator of a phase transition for deforming near-critical systems.

When a shear rate of 0.01 s^{-1} was applied to the melt in the one-phase region at 160 °C for 90 min, the SALS scattering pattern was independent of the shear strain, and it showed no evidence of shear-induced phase separation or stress-enhanced concentration fluctuations. Figure 3a shows the scattering pattern after 90 min (note that the light around the beam stop is caused by the main beam). Similarly, no structure was detected by TEM of samples sheared within the one-phase region.

When the temperature was increased from the one-phase region (160 °C) at a rate of 0.2 °C /min while shearing, an anisotropic light scattering pattern, Figure 3b, was detected at 175 °C or 7 °C above the quiescent cloud point. The seemingly straightforward explanation would be that stress had increased the phase separation temperature. If that hypothesis were correct, however, then no phase separation should occur below 175 °C if the same stress were used. But, that was not the case. When the same shear rate was applied to a sample being heated from 160 °C at the same heating rate and kept at 172 °C isothermally, an anisotropic scattering pattern appeared after shearing for 75 min. The coincidence of the time when phase separation started in both experiments (in both the isothermal and the dynamic heating experiments, phase separation occurred after 75 min of shearing at a rate of 0.01 s^{-1}) suggests that strain plays an important role in phase separation of near-critical blends under the influence of shear. The scattering pattern evolved from that with no scattering directly to an anisotropic, "two-wing" scattering pattern, without the typical spinodal ring pattern characteristic of spinodal decomposition of a quiescent blend. The "two-wing" scattering pattern corresponds to the chevron-like phase texture in real space. That result suggests that shear suppresses the concentration fluctuations in a near-critical polymer blend and the phase-separation process may follow a different mechanism than conventional spinodal decomposition.[18]

High-Stress Flows. The flow curve calculated from capillary viscometry of the 25/75 SAN/PMMA at 180 °C

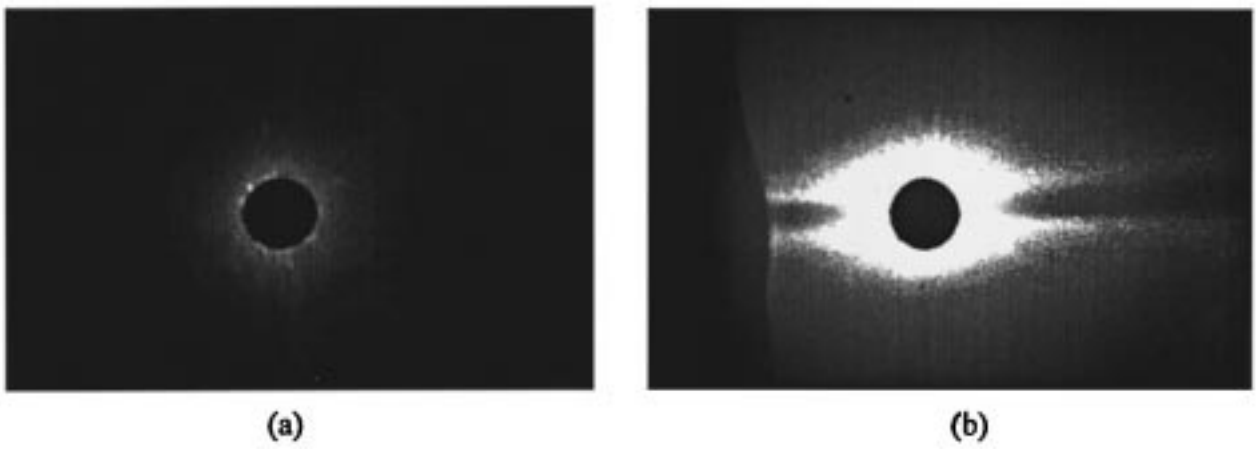

Figure 3. 2D light scattering patterns under a steady shear rate of 0.01 s^{-1}: (a) $T = 160$ °C, $\gamma = 54$; (b) $T = 175$ °C, $\gamma = 45$.

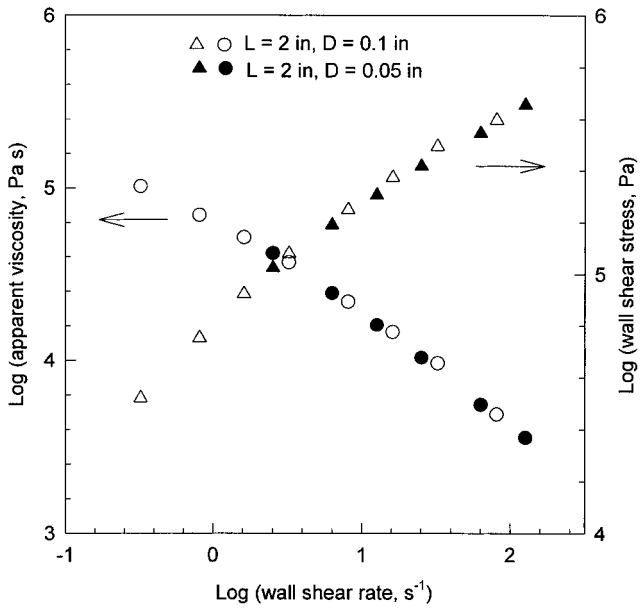

Figure 4. Stress and viscosity as functions of shear rate for 25/75 SAN/PMMA at 180 °C.

is shown in Figure 4. A flow instability occurred for wall shear stresses exceeding 452 kPa. Figure 5 shows TEM images of the blend after being extruded at a shear rate of 81 s^{-1} and a stress of 395 kPa. The residence time corresponding to the radius of the capillary extrudate at which the TEM's were taken was only 6 s, but the shear strain was 486. Figure 5 and other micrographs revealed that in the plane perpendicular to the flow (r, θ), phase domains remained interconnected with an average size of 0.18 μm (here, the size means the diameter of the drop normal to the flow direction). However, in the flow direction, the domains were significantly deformed and appeared fibrillar. These results are in stark contrast to those of Lyngaae-Jørgenson and Søndergaad,[5] who noted that "no structure was detected at stresses above approximately 100 kPa", for virtually the same blend as was used in our study.

Similar results were obtained in the modified normal-stress extruder. At a shear rate of 12 s^{-1}, corresponding to a shear stress of 202 kPa (residence time was ca. 100 s), the rapidly quenched sample exhibited a fibrillar structure in the flow direction, see Figure 6. This independent observation, again, is different from the results of Lyngaae-Jørgenson and Søndergaad.[5]

Hydrodynamic Explanation. A close examination of the microstructure of the SAN/PMMA blend after shear flow revealed that the phase-separated droplets had a wide size distribution. Some were large ellipsoids, some were small spheres, and some were on the verge of breaking. That description is very similar to the result of classical hydrodynamic behavior of immiscible liquids. The foundations of Newtonian droplet breakup under shear were established by Taylor,[27] who modeled drop size under simple shear flow using the viscosity ratio, $\eta_r = \eta_d/\eta_m$, and the Weber number, We:

$$We \equiv \frac{\dot{\gamma}\eta_m R}{\sigma} = \frac{\tau_{21} R}{\sigma} \tag{2}$$

where $\dot{\gamma}$ is the shear rate, η_m is the matrix phase viscosity, η_d is the dispersed phase viscosity, R is the radius of the drop, and σ is the interfacial tension. Taylor predicted that no drop breakup occurs when $\eta_r > 2.5$. For the SAN/PMMA blend system at 180 °C, η_r is 0.55, which yields a critical We[28] of about 1, and the interfacial tension is estimated to be ca. 0.5 mN/m. (Due to the lack of literature data and experimental difficulties in measuring the interfacial tension near the critical point, the estimated interfacial tension was calculated as described in the Appendix.) The drop size predicted by eq 2, i.e., the Taylor limit, is plotted against shear stress in Figure 7. A limitation of eq 2 is that it only applies for isolated Newtonian droplets, whereas the droplet concentration in a phase-separated melt blend is high. Polymer melts are also viscoelastic and the phase-separated droplets tend to elongate significantly before breaking. Therefore, in a phase-separated polymer blend, the droplet size is always greater than the Taylor limit at moderate shear rates.[29−33]

The experimental observations of Elmendorp and Van der Vegt,[29] Serpe et al.,[30] and Sundararaj and Macosko[31] of immiscible blends indicate that the droplet size is affected immensely by the concentration of dispersed phase and the elasticity of the drop. We can modify the Taylor prediction to apply to the experimental condition by applying the empirical equation proposed by Serpe et al.,[30]

$$\frac{D}{D_0} = \frac{1}{1 - (4\phi_d\phi_c)^{0.8}} \tag{3}$$

where D is the diameter of the drop, D_0 is the diameter of the drop at zero concentration, and ϕ_d and ϕ_c are the

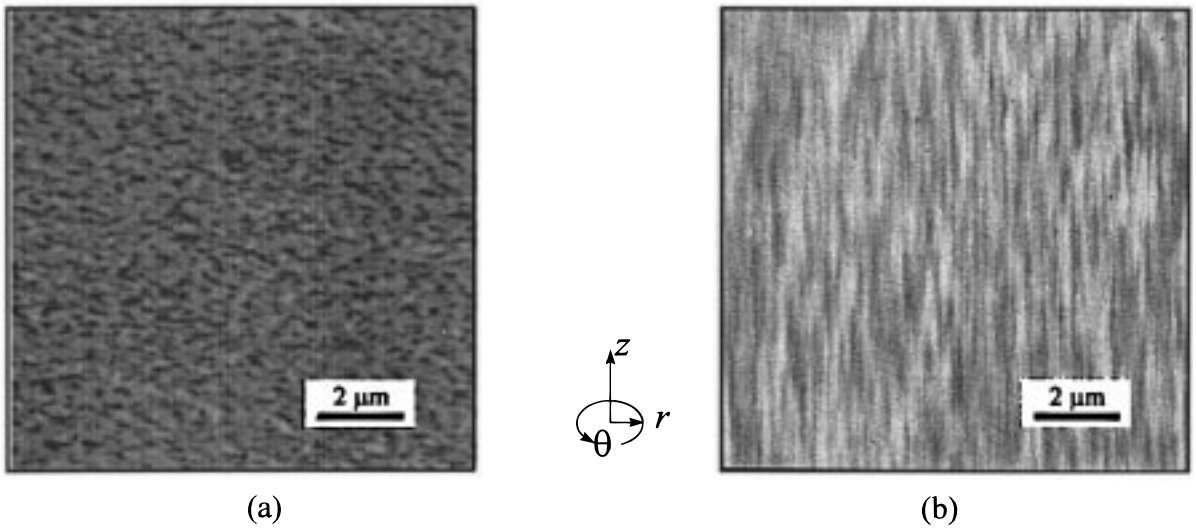

Figure 5. Morphology of 25/75 SAN/PMMA after being sheared at 81 s^{-1} (τ = 395 kPa) and quenched: (a) r, θ plane; (b) r, z plane (z is the flow direction).

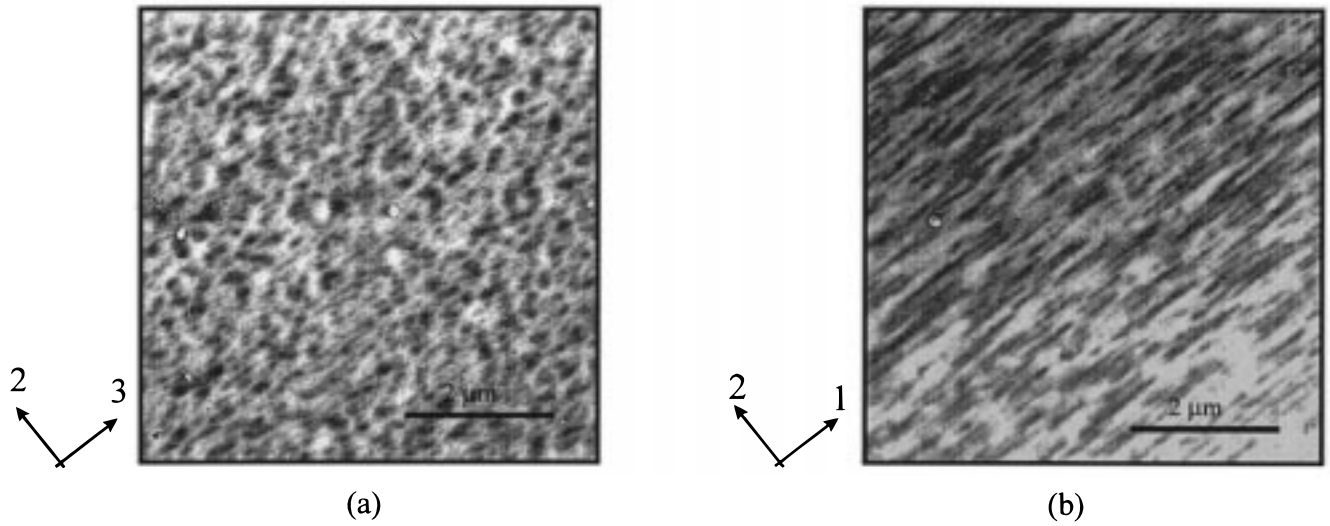

Figure 6. Morphology of 25/75 SAN/PMMA after being sheared in the normal-stress extruder at 12 s^{-1} (τ = 202 kPa) and quenched: (a) 2−3 plane; (b) 1−2 plane (1 is the flow direction; 2 is the gradient direction).

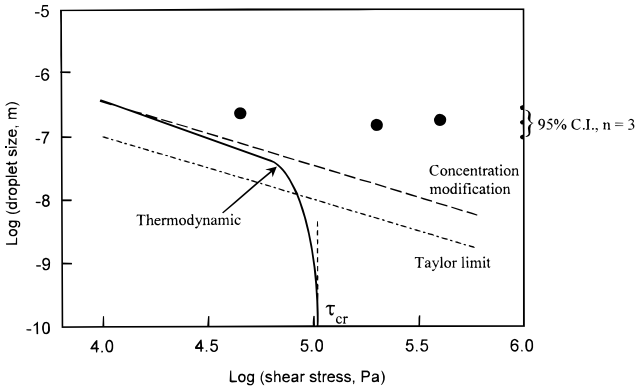

Figure 7. Size−stress relationship for polymer blends under shear. The solid line is the schematic representation of thermodynamic theory (the critical shear stress is adopted from ref 5, note that before stress reaches the critical value, the droplet size is expected to behave the same as what hydrodynamic theory predicts).

concentration of dispersed phase and continuous phase, respectively. Figure 7 compares the predictions of eq 3 (the dashed line marked concentration modification) with the Taylor limit (eq 2) using the parameters for the SAN/PMMA system. Equation 3 predicts a drop size that is ca. 3.3 times larger than the Taylor limit. The three points shown in Figure 7 are shear-induced drop sizes estimated from the conditions corresponding to our three independent experimental techniques, rheo-SALS, the normal-stress extruder, and the Instron capillary rheometer, for which the shear stress ranged from 20 to 450 kPa. The 95% confidence interval of the average drop size for these three data points is also depicted in the figure. The results show that the drop size does not vary much at high shear stress. While the thermodynamic theory (solid line, Figure 7) predicts that the dispersed phase disappears when the shear stress exceeds a critical value, the size of the domains in our experiment tended to reach an equilibrium size under the combined influence of the shear field, elastic forces, and interfacial tension. The classic droplet breakup theory also does not predict quantitatively the size of viscoelastic droplets under high shear stress. This may be explained as follows. When shear is applied to the phase-separated blend, the matrix viscous forces build and deform the drop. Steady state deformation

of the drop is achieved when the interfacial forces and the elasticity resisting the deformation exactly balance the viscous forces. Since N_1 invariably varies with τ_{21} to a power higher than 1, the elastic effects dominate at high shear rates. The rate of agglomeration increases with the increasing shear rate.[31,32] Therefore, at high shear stresses, the drop size in a viscoelastic system tends to reach steady state at droplet sizes much higher than what Taylor predicts.

Conclusion

The structural changes and phase behavior of a near-critical blend, SAN/PMMA, under the influence of shear were studied. When shear was applied to a phase-separated blend, the structure of phase domains evolved from bicontinuous to chevron-like, and finally to fibrillar. The unique chevron structure was tentatively associated with the high interconnectivity of the material and low interfacial energy. No shear-induced phase transition was detected. When the blend was subjected to high stresses (above 100 kPa), the domain structure was highly oriented in the flow direction, yet remained interconnected in the direction perpendicular to the flow. The flow-induced structural changes were qualitatively explained in terms of hydrodynamic effects.

Acknowledgment. This work was supported by a grant from the Polymer Compatibilization Research Consortium at the University of Connecticut. We thank Dr. M. Cantino and Ms. L. Khairallah for performing TEM and Dr. G. Dee for the help with the calculation of the interfacial tension. PMMA and SAN samples were kindly provided by ICI Acrylics Corp. and Dr. A. Padwa from Bayer Corp., respectively.

Appendix. Estimation of the Interfacial Tension of the SAN/PMMA Blend

The interfacial tension between two polymers can be estimated using a harmonic-mean equation,[34]

$$\sigma_{12} = \sigma_1 + \sigma_2 - \frac{4\sigma_1^{\,d}\sigma_2^{\,d}}{\sigma_1^{\,d} + \sigma_2^{\,d}} - \frac{4\sigma_1^{\,p}\sigma_2^{\,p}}{\sigma_1^{\,p} + \sigma_2^{\,p}} \qquad (4)$$

where σ_{12} is the interfacial tension between components 1 and 2, σ_i is the surface tension of the ith component, $\sigma_i^{\,p}$ is the polar surface tension and $\sigma_i^{\,d}$ is equal to ($\sigma_i - \sigma_i^{\,p}$). The polar surface tension is defined as

$$\sigma_i^{\,p} = x_i^{\,p}\sigma_i \qquad (5)$$

where $x_i^{\,p}$ is the polarity.

The surface tension for SAN with 25 wt % AN content can be predicted by using the dimensional equation

$$\sigma_{SAN}\ (\text{mN/m}) = 40.36 - 0.07456T\ (^\circ\text{C}) \qquad (6)$$

(This equation is based on the calculation using the equation of state for styrene-*co*-acrylonitrile by Dr. Greg Dee at E. I. Dupont de Nemours & Co.) Therefore, at 180 °C, $\sigma_{SAN} = 26.94$ mN/m. At this point, there are no available data for SAN29. We applied the data for SAN25 in the later calculation. The polarity of polystyrene and polyacrylonitrile are 0.168 and 0.251, respectively.[34] By assuming the molar linear relationship for polarity of a random copolymer, $x_{SAN}^{\,p}$ is calculated to be 0.205. From the literature,[34] σ_{PMMA} at 180 °C is 28.94 mN/m and $x_{PMMA}^{\,p}$ is 0.280. Substituting the values in eq 5, we obtained the interfacial tension of SAN and PMMA at 180 °C as 0.49 mN/m. For a near-critical blend, one would expect low interfacial tension. Also, compared with the 0.3 mN/m that was estimated by McMaster,[22] the number seems to be reasonable.

References and Notes

(1) *Flow-Induced Structure in Polymers*; Nakatani, A., Dadmun, M. D., Eds.; American Chemical Society: Washington, DC, 1995.
(2) Silberberg, A.; Kuhn, W. *Nature* **1952**, *170*, 450.
(3) Mazich, K. A.; Carr, S. H. *J. Appl. Phys.* **1983**, *54*, 5511.
(4) Katsaros, J. D.; Malone, M. F.; Winter, H. H. *Polym. Bull.* **1986**, *16*, 83.
(5) Lyngaae-Jorgenson, J.; Sondergaard, K. *Polym. Eng. Sci.* **1987**, *27*, 351.
(6) Cheikh Larbi, F. B.; Malone, M. F.; Winter, H. H.; Halary, J. L.; Leviet, M. H.; Monnerie, L. *Macromolecules* **1988**, *21*, 1.
(7) Rector, C. M.; Mazich, K. A.; Carr, S. H. *J. Macromol. Sci., Phys.* **1988**, *B27*, 421.
(8) Katsaros, J. D.; Malone, M. F.; Winter, H. H. *Polym. Eng. Sci.* **1989**, *29*, 1434.
(9) Nakatani, A. I.; Kim, H.; Takahashi, Y.; Matsushita, Y.; Takano, A.; Bauer, B. J.; Han, C. C. *J. Chem. Phys.* **1990**, *93*, 795.
(10) Mani, S.; Malone, M. F.; Winter, H. H.; Halary, J. L.; Monnerie, L. *Macromolecules* **1991**, *24*, 5451.
(11) Kammer, H. W.; Kummerloewe, C.; Kressler, J.; Meliot, J. P. *Polymer* **1991**, *32*, 1488.
(12) Hindawi, I. A.; Higgins, J. S.; Weiss, R. A. *Polymer* **1992**, *33*, 2522.
(13) Mani, S.; Malone, M. F.; Winter, H. H. *Macromolecules* **1992**, *25*, 5671.
(14) Fernandez, M. L.; Higgins, J. S. *Polym. Mater. Sci. Eng.* **1994**, *71*, 39.
(15) Fernandez, M. L.; Higgins, J. S.; Horst, R.; Wolf, B. A. *Polymer* **1995**, *36*, 149.
(16) Hindawi, I.; Higgins, J. S.; Galambos, A. F.; Weiss, R. A. *Macromolecules* **1990**, *23*, 670−674.
(17) Han, C. C. *Macromol. Symp.* **1996**, *101*, 157−165.
(18) Matsuzaka, K.; Jinnai, H.; Koga, T.; Hashimoto, T. *Macromolecules* **1997**, *30*, 1146−1152.
(19) Douglas, J. F. *Macromolecules* **1992**, *25*, 1468−1474.
(20) Chen, Z. J.; Wu, R.-J.; Shaw, M. T.; Weiss, R. A.; Fernandez, M. L.; Higgins, J. S. *Polym. Eng. Sci.* **1995**, *35*, 92.
(21) Chen, Z. J.; Shaw, M. T.; Weiss, R. A. *Macromolecules* **1995**, *28*, 648.
(22) McMaster, L. P. *Macromolecules* **1973,** *6*, 760.
(23) Moonay, D. J.; Wu, R. J.; Shaw, M. T. *Proc. Soc. Plastics Eng., ANTEC* **1994**, II, 2038.
(24) Wu, R.; Shaw, M. T.; Weiss, R. A. *Polym. Mater. Sci. Eng.* **1993**, *68*, 264.
(25) Hashimoto, T.; Matsuzaka, K.; Kume, T.; Moses, E. *Polym. Mater. Sci. Eng.* **1994**, *71*, 111.
(26) Hashimoto, T.; Matsuzaka, K.; Moses, E.; Onuki, A. *Phys. Rev. Lett.* **1995**, *74*, 126.
(27) Taylor, G. I. *Proc. R. Soc. London* **1934**, *A146*, 501.
(28) Grace, H. P. *Chem. Eng. Commun.* **1982**, *14*, 225.
(29) Elmendorp, J. J.; van der Vegt, A. K. *Polym. Eng. Sci.* **1986**, *26*, 1332.
(30) Serpe, G.; Jarrin, J.; Dawans, F. *Polym. Eng. Sci.* **1990**, *30*, 553.
(31) Sundararaj, U.; Macosko, C. W. *Macromolecules* **1995**, *28*, 2647.
(32) Ghodgaonkar, P. G.; Sundararaj, U. *Polym. Eng. Sci.* **1996**, *36*, 1656−1665.
(33) Grizzuti, N.; Bifulco, O. *Rheol. Acta* **1997**, *36*, 406−415.
(34) Wu, S. *Polymer interface and adhesion*; Marcel Dekker: New York, 1982.

MA980637R